2021 IEEE 17th International Conference on Group IV Photonics (GFP) | 978-1-6654-2224-6/21/$31.00 ©2021 IEEE | DOI: 10.1109/GFP51802.2021.9673887

Multi-level Encoding and Decoding in a Wavelength-Multiplexed Photonic Tensor Processor

Zhimu Guo[1], Bicky A. Marquez
Matthew Filipovich, Hugh Morison
and Bhavin J. Shastri[†‡2]
[†]Department of Physics, Engineering
Physics and Astronomy
Queen's University
Kingston, ON K7L 3N6, Canada

Lukas Chrostowski
and Sudip Shekhar
Department of Electrical and
Computer Engineering
University of British Columbia
Vancouver, British Columbia
V6T 1Z4, Canada

Paul Prucnal[‡]
[‡]Department of Electrical Engineering
Princeton University
Princeton, NJ 08544, USA

***Abstract*—Photonic processors have enabled applications in machine learning and neuromorphic computing. An information encoding/decoding scheme will be critical for scalable photonic computing. We experimentally demonstrate a "multi-level" encoding/decoding scheme and operation procedures.**

I. Introduction

Recent advancements in dedicated photonic processors for various machine learning tasks have seen an increasing demand for a structured photonic programming scheme for efficient communication between photonic hardware and its control system[1], [2], [3], [4]. The core of a programming scheme is an information encoding and decoding method that translates the same information between different hardware platforms using their "languages" respectively.

In this work, we present a feasible information encoding/decoding solution for microring resonator (MRR) based photonic architecture[5], [6] as shown in Fig. 1. Here, the photonic tensor processing element (TPE) includes an array of five MRRs in an add/drop configuration and are coupled with two bus waveguides—a shared waveguide for IN-THRU connection, and another one connecting the DROP. Five lasers are used to provide inputs for the MRRs using different wavelengths respectively. The input optical power is redistributed between the DROP and the THRU ports according to the difference between the resonant wavelength of the MRR and the laser controlled by shifting the resonant wavelength of the MRR using thermo-optical effect[7], [8] or using phase-change materials[9].

The TPE control system consists of five current sources and a powermeter with a . The current sources provide currents to the MRRs that use the thermo-optical effect to cause a resonance shift. The powermeter and the balanced photodetector collects output optical powers from both DROP and THRU ports and subtracts the THRU port power from the DROP port power, giving us $P_{DROP} - P_{THRU}$ in units of dB[10]. All analog values are passed to and from the computer that regulates the information flow between a user application for machine learning and the photonic TPE.

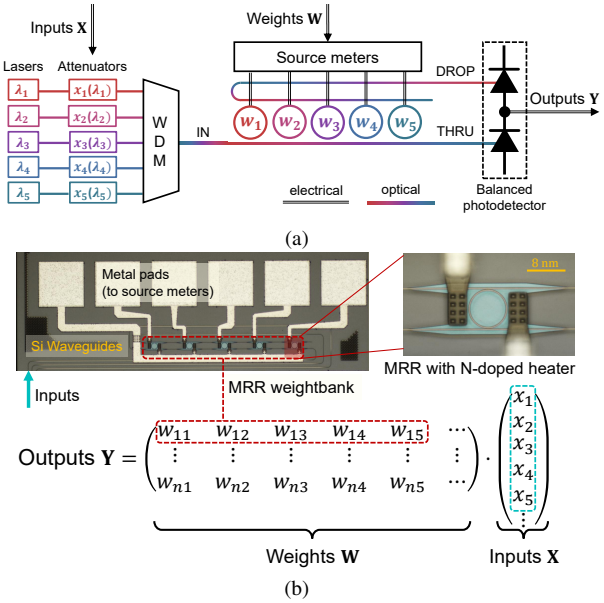

Fig. 1: (a): schematics of an MRR-based photonic TPE for 5-element vector dot product between vectors $\mathbb{X}$ and $\mathbb{W}$, along with its control system. (b): general mathematical concept for matrix-vector dot product using MRRs, and an optical micrograph of the fabricated silicon photonic TPE on a silicon-on-insulator (SOI) platform.

II. Information Encoding and Decoding

The proposed "multi-level" scheme is an information encoding/decoding scheme used on the photonic TPE shown above. The encoding scheme requires each photonic channel to represent numbers with n-bit precision using analog signals, and every analog value to be decoded back to its corresponding digital value. The photonic TPE has already shown promising results in its bit precision, and the highest possible precision achieved on a single photonic channel has been verified to be 7-bit[11], and more recently to be 8.52-bit[12].

[1]Email: 15zg11@queensu.ca
[2]Also at Vector Institute, Toronto, ON M5G 1M1, Canada.

978-1-6654-2224-6/21/$31.00 ©2021 IEEE

A direct value mapping is implemented to translate digital numbers to analog values, and calibration and validation stages are also required. The calibration stage first starts with encoding the inputs to the MRR as the amplitude of the input optical channel modulated by an attenuator. Here, a direct *input mapping* encodes digital input values as the attenuation applied on the input optical channel. Next, we perform a current sweep for one MRR at a time using a constant laser power, and a linear response in optical output power, $P_{DROP} - P_{THRU}$, is chosen as the *MRR profile*, as shown in Fig. 2(a). Now we need to define the *zero point*, or the *reflection point*, of the MRR, which can be interpreted as the specific current value required to evenly distribute an output optical power between DROP and THRU ports. This ensures the power difference between the two ports is essentially a constant regardless of the input power. Thus, we perform a two-dimensional sweep on both the current and input optical power to find the reflection point for the MRR. Combining the *reflection point* and the *MRR profile*, a *weight mapping* is created between the digital values and analog currents provided to the MRR. The *output mapping* generates random numbers for both the MRR and the laser, and the product of the two represents the expected output. The measured outputs from the MRR are mapped to the range of desired digital values after a linear regression as shown in Fig. 2(b). Here, we use a 6-bit system with 5-bit inputs for demonstration.

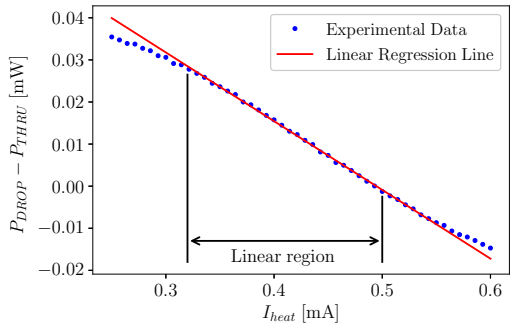

(a)

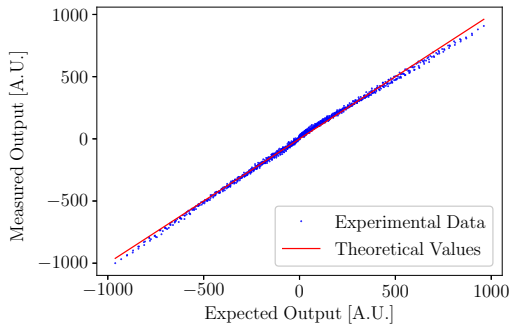

(b)

Fig. 2: Experimental data for (a) the MRR profile mapping the measured output to the applied current, and (b) the output mapping between measured and expected outputs for a 6-bit system.

III. Discussion

a) ***Precision flexibility****:* The multi-level scheme only provides finite precision for number representation, but the range of user requested values can vary depending on the specific application intended for the photonic TPE. However, since the direct value mapping between digital values and the analog values is arbitrary, the photonic TPE can switch between different bit-precision only requiring a system re-calibration. Therefore, the photonic TPE can be flexible with its bit-precision during the encoding and decoding process.

b) ***Negative number encoding****:* The input encoding for both the MRRs and the attenuators uses the same direct value mapping between digital and analog values, but the underlying operating mechanisms are different. For the attenuators, different digital values are mapped to different optical power amplitudes, resulting in an always-positive analog input. For the MRRs, the digital values are mapped to the applied current values, and depending on whether the value is larger or smaller than the reflection point current value, the output of the MRR can either be positive or negative. Therefore, the input mapping can only encode positive numbers, whereas the weight mapping encodes both positive and negative numbers. The multi-level encoding scheme will encode all negative numbers as weights during multiplication, and cases involving two negatives are treated as two positives.

IV. Conclusion

We have demonstrated the proposed "multi-level" encoding/decoding scheme for a MRR-based photonic TPE, and the experimental results have verified its feasibility. We have also noted some unique characteristics of the photonic TPE architecture, and by taking advantages of its flexibility we have refined and improved the details of the multi-level scheme. Using this encoding/decoding scheme as the operation foundation will allow us to explore more machine learning applications for MRR-based photonic TPEs.

References

[1] P. Prucnal *et al.* CRC Press, Jan. 2017.
[2] B. J. Shastri *et al.*, *arXiv:2011.00111*, 2020.
[3] Y. Shen *et al.*, *Nature photonics*, vol. 11, no. 7, pp. 441–446, 2017.
[4] J. Feldmann *et al.*, *Nature*, vol. 589, no. 7840, pp. 52–58, Jan 2021. [Online]. Available: https://doi.org/10.1038/s41586-020-03070-1
[5] A. N. Tait *et al.*, *Scientific reports*, vol. 7, no. 1, pp. 7430–10, 2017.
[6] V. Bangari *et al.*, *IEEE Journal of Selected Topics in Quantum Electronics*, vol. 26, no. 1, pp. 1–13, 2020.
[7] A. N. Tait *et al.*, *Opt. Express*, vol. 26, no. 20, pp. 26 422–26 443, Oct 2018. [Online]. Available: http://www.opticsexpress.org/abstract.cfm?URI=oe-26-20-26422
[8] L.-W. Luo *et al.*, *Optics letters*, vol. 37, no. 4, pp. 590–592, 2012. [Online]. Available: http://search.proquest.com/docview/922501124/
[9] J. Feldmann *et al.*, *Nature*, vol. 569, no. 7755, pp. 208–214, May 2019. [Online]. Available: https://doi.org/10.1038/s41586-019-1157-8
[10] M. S. Hai *et al.*, *Opt. Express*, vol. 21, no. 26, pp. 32 680–32 689, Dec 2013. [Online]. Available: http://www.opticsexpress.org/abstract.cfm?URI=oe-21-26-32680
[11] C. Huang *et al.*, *APL Photonics*, vol. 5, no. 4, p. 040803, 2020. [Online]. Available: https://doi.org/10.1063/1.5144121
[12] W. Z. *et al.*, *arXiv:2104.01164*, 2021.